The Journal of Neuroscience, May 15, 1997, 17(10):3379–3391

Frequency-Dependent Inactivation of Mammalian A-Type K^+ Channel $K_V1.4$ Regulated by Ca^{2+}/Calmodulin-Dependent Protein Kinase

Jochen Roeper, Christoph Lorra, and Olaf Pongs

Zentrum für Molekulare Neurobiologie, Martinistrasse 52, D-20246 Hamburg, Germany

Ca^{2+}/calmodulin dependent protein kinase (CaMKII) and protein phosphatase 2B (calcineurin) are key enzymes in the regulation of synaptic strength, controlling the phosphorylation status of pre- and postsynaptic target proteins. Here, we show that the inactivation gating of the *Shaker*-related fast-inactivating K_V channel, $K_v1.4$ is controlled by CaMKII and the calcineurin/inhibitor-1 protein phosphatase cascade. CaMKII phosphorylation of an amino-terminal residue of $K_V1.4$ leads to slowing of inactivation gating and accelerated recovery from N-type inactivated states. In contrast, dephosphorylation of this residue induces a fast inactivating mode of $K_V1.4$ with time constants of inactivation 5 to 10 times faster compared with the CaMKII-phosphorylated form. Dephosphorylated $K_V1.4$ channels also display slowed and partial recovery from inactivation with increased trapping of $K_V1.4$ channels in long-absorbing C-type inactivated states. In consequence, dephosphorylated $K_V1.4$ displays a markedly increased tendency to undergo cumulative inactivation during repetitive stimulation. The balance between phosphorylated and dephosphorylated $K_V1.4$ channels is regulated by changes in intracellular Ca^{2+} concentration rendering $K_V1.4$ inactivation gating Ca^{2+}-sensitive. The reciprocal CaMKII and calcineurin regulation of cumulative inactivation of presynaptic $K_V1.4$ may provide a novel mechanism to regulate the critical frequency for presynaptic spike broadening and induction of synaptic plasticity.

Key words: voltage-activated K channels; Shaker*; N-type inactivation; C-type inactivation; phosphorylation; CaMKII; calcineurin; protein phosphatase; synapse*

The strength of synaptic connections within neuronal circuits is flexible. This plasticity in neuronal excitability has been recognized as an important property underlying short- and long-term changes in the concerted activity of pre- and postsynaptic elements including ion channels (Kandel et al., 1991; Bliss and Collingridge, 1993; Zucker, 1993). It has been shown for a number of ligand- and voltage-gated ion channels that their activity can be modulated by the activation of protein kinases and phosphatases, which are regulated, in turn, by second messenger systems, e.g., Ca^{2+} and cAMP (Schulman, 1995). Potassium channels that constitute an extremely diverse superfamily involved in the control of pre- and postsynaptic excitability in this respect are particularly interesting. The regulation of potassium channel activity by protein phosphorylation may alter very distinctly neuronal excitability (Jonas and Kaszmarek, 1996).

Several recent *in vitro* studies have focused on the *Shaker* superfamily of voltage-activated potassium (K_V) channels (Chandy and Gutman, 1994). It was shown that phosphorylation by protein tyrosine kinase reduced the activity of $K_V1.2$ and $K_V1.3$ channels (Huang et al., 1993; Lev et al., 1995; Holmes et al., 1996). Also, cAMP-dependent protein kinase A (PKA) phosphorylation upregulates the activity levels of $K_v1.2$ (Huang et al., 1994) and $K_V2.1$ (Wilson et al., 1994) and downregulates that of $K_V3.2$ channels (Moreno et al., 1995). These K_V channels belong to the class of delayed-rectifier channels mediating currents that do not inactivate rapidly. Other *Shaker*-related K_V channels, e.g., *Shaker* itself, $K_V1.4$, and $K_V3.4$, express outward currents that rapidly inactivate within milliseconds because of the presence of an amino-terminal inactivation domain (Hoshi et al., 1990). It was shown that phosphorylation of the amino-terminal inactivation domain of $K_V3.4$ channels by protein kinase C (PKC) completely eliminated N-type inactivation (Covarrubias et al., 1994). Also, dephosphorylation of a modulatory C-terminal site of *Drosophila Shaker* channels considerably slowed the inactivation rate (Drain et al., 1994).

Ca^{2+}/calmodulin-dependent kinases (CaMKIIs) are prominently expressed in mammalian brain, both pre- and postsynaptically. It is well accepted that CaMKII, which phosphorylates several pre- and postsynaptic proteins, has an important function in regulating neuronal excitability and synaptic strength (Braun and Schulman, 1995). It has been shown that members of the *Shaker* K_V channel family, e.g., K_V 1.1, K_V 1.2, and K_V 1.4, are localized to pre- and postsynaptic compartments (Sheng et al., 1992, 1993; Veh et al., 1995), making them possible targets for CaMKII phosphorylation. When we screened the cytoplasmic regions of $K_V1.4$, a rapidly inactivating K_V channel (Stühmer et al., 1989), for possible CaMKII phosphorylation sites, we detected three CaMKII consensus sequence motifs in the cytoplasmic amino-terminal sequence (RXXS/T at serine 101/102 and 123, and threonine 191). We show here that serine 123 of $K_V1.4$ is a substrate for CaMKII phosphorylation and that CaMKII-phosphorylated K_V 1.4 channels are dephosphorylated by the Ca^{2+}-regulated calcineurin (protein phosphatase 2B)/inhibitor-1 protein phosphatase cascade. This Ca^{2+}-sensitive phosphorylation/dephosphorylation of K_V 1.4 has profound functional consequences for the

Received Aug. 10, 1996; revised Feb. 18, 1997; accepted Feb. 24, 1997.

This work was supported by a Grant of the Deutsche Forschungs-gemeinschaft (O. P.). We thank D. Clausen for excellent graphical services, S. Sewing for help with *in vitro* mutagenesis, and D. Kuhl and C. Stansfeld for critical reading of the manuscript.

Correspondence should be addressed to Dr. Olaf Pongs, Zentrum für Molekulare Neurobiologie, Martinistrasse 52, D-20246 Hamburg, Federal Republic of Germany.

Dr. Lorra's present address: Institut für Neurobiologie; INF 364, 69120 Heidelberg, Germany.

 0270-6474/97/173379-13$05.00/0

inactivation properties of K_V 1.4-mediated A-type potassium currents.

MATERIALS AND METHODS

Construction of HEK 293-K_V1.4 cell line. Briefly, rat K_V1.4 cDNA nucleotide (nt) 387–2658 (Stühmer et al., 1989) subcloned into pBluescript pKS^+ was combined with a blunt-end Ear I fragment of the metallothionein II_A promotor (MT) [nt 30–830; (Karin et al., 1984)] cloned into the *Sal*I polylinker restriction site of Bluescript pKS^+. The resulting K_V1.4 pKS^+ clone was digested with *Eco*RI/*Bgl*II. The isolated *Eco*RI/*Bgl*II MT-K_V1.4 restriction fragment was ligated with *Eco*RI/*Bgl*II cut pML2 eucariontic expression vector, containing polyadenylation and transcription termination signals from the SV40 late region. The K_V1.4 pTMT-construct was checked by restriction analysis. HEK 293 cells were transfected with K_V1.4 pTMT DNA after the protocol of Chen and Okayama (Chen et al., 1987). HEK 293 cells were grown in DMEM:F12 (Life Technologies, Gaithersburg, MD) supplemented with 10% FCS (Biother), 2 mM L-glutamine (Life Technologies) and penicillin-streptomycin (50 IU/ml-50 μg/ml; Life Technologies). Stably transfected cells were selected with 1 mgl G418 (Life Technologies). Selected HEK 293-K_V1.4 cell clones were analyzed by Northern blot analysis for K_V1.4 RNA expression and by Western blot analysis for K_V1.4 protein expression.

In vitro *Mutagenesis.* Point mutations in the K_V1.4 amino terminus were introduced by a PCR-based site-directed mutagenesis (Ho et al., 1989). For the mutation K_V1.4 S123A we used the following oligonucleotides: AAG ATC CTT AGG GAG *ATG GCC* GAG GAG GAG (sense) and GTG GTA GAA AAT AGT TAA A (antisense). The PCR products were digested with *Sau*I and ligated into K_V1.4 pAKS2. The mutant K_V1.4 T191A was generated by an overlay PCR using the oligonucleotides CTA CGC TTC GAA *GCC* CAA ATG AAA (sense) and TTT CAT TTG *GGC* TTC GAA GCG TAG (antisense). The two PCR fragments were digested with *Sau*I and cloned into K_V1.4 pAKS2. The mutant Kv 1.4 SS101/102AA was generated by using oligonucleotides CAC AGG CAG *GCC GCT* TTT CCT CAT TGC (sense) and G AGG AAA *AGC GGC* CTG CCT GTG GTG GAG (antisense). The product from the overlap PCR was cut with *Nco*I and cloned into Kv1.4 pAKS2. All mutants were verified by sequencing (Sanger et al., 1977) before use. For mRNA synthesis K_V1.4 pAKS2, K_V1.4 S123A pAKS2, and K_V1.4 T191A pAKS2 were linearized with *Eco*RI. *In vitro* transcription was performed using the Sp6 Message Machine (Ambion, Austin, TX).

In vitro *translation and* in vitro *phosphorylation.* The radioactive *in vitro* translation of K_V1.4 pAKS2 and K_V1.4 S123A were performed using 1 μg cRNA in the FLEXI rabbit reticulocyte lysate system (Promega, Madison, WI) with ^{35}S-methionine according to protocol. The reactions (final volume, 50 μl) were incubated for 1 hr at 30°C in the presence of 7.2μ canine pancreatic microsomal membranes. For *in vitro* phosphorylation, nonradioactive *in vitro* translation was set up using a full amino acid mixture and incubated under the same conditions as above. The microsomal membranes were sedimented at 4°C with an Eppendorf (Madison, WI) tabletop centrifuge at 15,300 rpm and afterward resuspended in CAMKII reaction buffer (20 mM Tris/HCl, pH 7.5, 10 mM $MgCl_2$, 2 mM $CaCl_2$, 0.5 mM dithiothreitol, 0.1 mM EDTA). For *in vitro* phosphorylation, 2.4 μM calmodulin, 100 μM ATP, ^{32}P-γ-ATP (specific activity of 100 μCi/μmol) and 250 U CaMKII (New England Biolabs, Beverly, MA) were added to the mixture. The reactions (final volume, 50 μl) were incubated at 30°C for 10 min in the presence of 1 mM Cyclosporin A and 100 μM okadaic acid. The reactions were stopped by addition of 50 μl of prewarmed (56°C) 2× Laemmli buffer. Ten microliters of the *in vitro* translation and 20 μl of the *in vitro* phosphorylation reaction were loaded per lane on 10% SDS-polyacrylamide gels. For control, *in vitro* translation and phosphorylation reactions without cRNA were performed to estimate the background of the *in vitro* phosphorylation reaction.

Electrophysiology and microinjection. Macroscopic currents were obtained from perforated-patch (Rae et al., 1991) and standard whole-cell patch-clamp recording (Hamill et al., 1981) using HEK 293-K_V1.4 cells and cRNA-microinjected 293 cells. They were maintained with standard cell culture protocols and plated at a density of 5×10^4/ml on poly-L-lysine (50 μg/ml)-coated cellocate grids (Eppendorf) 1 d before the experiment. The bath solution for electrophysiological experiments contained (in mM): 135 NaCl, 5 KCl, 2 $CaCl_2$, 2 $MgCl_2$, 5 HEPES, 10 glucose, 20 sucrose, pH = 7.4 with NaOH. For perforated-patch recordings, the pipette solution contained (in mM): 70 K_2SO_4, 10 KCl, 10 NaCl, 7 $MgCl_2$, 10 HEPES, pH = 7.2 with KOH, and 0.25 mg/ml amphotericin-B. For standard whole cell, the pipette solution contained (in mM): 95 K-aspartate, 20 KCl, 1 $CaCl_2$, 11 EGTA, 10 HEPES, 2 glutathione, 2 Na_2ATP, pH = 7.2 with KOH with a calculated (EQCAL, Biosoft, Cambridge, UK) free Ca^{2+} concentration of 20 nM. Total $CaCl_2$ concentrations were increased according to EQCAL calculations to obtain free Ca^{2+} concentrations between 100 and 1000 nM. Patch pipettes were pulled from borosilicate glass with resistances between 2 and 4 MΩ. Only standard whole-cell experiments with series resistances <10 MΩ and perforated-patch experiments with <15 MΩ were included in this study. Series resistance compensation (0–80%) was used to obtain voltage errors <5 mV. Currents were recorded with an EPC9 (HEKA Elektronik) patch-clamp amplifier. The program package PULSE + PULSEFIT (HEKA Elektronik) was used for data acquisition and analysis. Leakage and capacitive currents were subtracted on-line using the P/4 subtraction method. P/4 pulses were applied 2 sec after the test pulses and the interpulse intervals were 30 sec. Records were digitized at 5 kHz and filtered with low-pass Bessel characteristic of 1 kHz cut-off frequency. For quantification of the time course of K currents, individual sweeps were fitted with a Hodgkin–Huxley related formalism (PULSEFIT): $I = I^0 m(t)^4 h t$) with $m(t) = 1\text{-exp}(-t/t_m)$ and $h(t) = h_\infty + a1a2\ \exp(-t/t_{h1}) + (1-a1a2)\ \exp(-t/t_{h2})$. The time constants t_m t_{h1}, and t_{h2} determine the activation and inactivation kinetics, respectively, h_∞ the steady-state inactivation. The two inactivation time constants are weighted by the variable $a1/a2$. Steady-state activation and inactivation curves were fitted with Boltzmann functions and time courses of recovery with monoexponential functions using a Marquardt-Levenberg algorithm in SIGMAPLOT (Jandel Scientific, San Rafael, CA). All experiments were performed at 30 ± 0.5°C. Data are given as mean ± SEM.

Autothiophosphorylation of purified CaMKII from rat brain (Calbiochem, La Jolla, CA) was induced by 5 min incubation (25°C) of 2 μg/ml CaMKII with 30 mg/ml calmodulin, 50 mM ATP gm-S, and 1 mg/ml BSA in a solution containing (in mM): 50 HEPES; 5 $MgCl_2$; 0.3 $CaCl_2$, pH 7.4. Aliqouts of CaMKII-solution were dialyzed on microdialysis membranes (Millipore, Bedford, MA) against a 150 mM KCl + 10 mM HEPES, pH 7.4, solution for 30 min at 4 C° and subsequently microinjected in 293 cells. Calcineurin autoinhibitory peptide [(CNIP) Bachem, Torrance, CA) was dissolved in water and microinjected. Stock solutions of KN-62 and KN-93, okadaic acid (Calbiochem), and cylosporin A (Calbiochem) were dissolved in dimethylsulfoxide.

For microinjection of mRNA, CaMKII or CNIP, K_V1.4–293 or 293 cells were plated on poly-L-lysine-coated cellocate grids, and the Microinjector 5242 (Eppendorf) with an Automated Injection System (AIS) from Zeiss (Thornwood, NY) was used with solutions containing 50 ng/ml mRNA (Ikeda et al., 1992). K_V1.4 wild-type and mutant cDNAs were cloned into pAKS expression vector for *in vitro* mRNA synthesis as described (Stühmer et al., 1989). Appropriate filling of individual cells was obtained with injection times of 200–300 msec and injection pressures between 80 and 140 hPa. In initial experiments, the filling of HEK 293-K_v1.4 cells was verified by co-injection of 0.1% fluorescein isothiocyanate-Dextran [(Sigma, St. Louis, MO) data not shown].

RESULTS

K_V1.4 A-type currents in stably transfected 293 cells

Two hundred ninety-three cells were used as an *in vitro* model system to characterize the modulation of K_V1.4 currents by CaMKII and protein phosphatases. The cells were stably transfected with a rat K_V1.4 cDNA construct under control of the human metallothionin promoter (K_v1.4–293). K_V1.4–293 cells gave rise to voltage-activated rapidly inactivating outward currents (Fig. 1*A*). They had properties similar to K_V1.4 currents expressed previously in the *Xenopus* oocyte expression system (Stühmer et al., 1989). In the perforated-patch whole-cell configuation, depolarization of K_V1.4–293 cells to +40 mV produced K_V1.4 current amplitudes in the 1–10 nA range. For comparison, amplitudes of slowly activating, noninactivating endogeneous outward currents were at +40 mV in the 50–300 pA range in both control and K_V1.4–293 cells (data not shown). In our standard conditions, <5% of total outward current amplitude was attributable to endogenous 293 K channels. Activation of K_V1.4 currents in K_V1.4–293 cells was fast (time rise to peak <5 msec) and had a threshold at approxi-

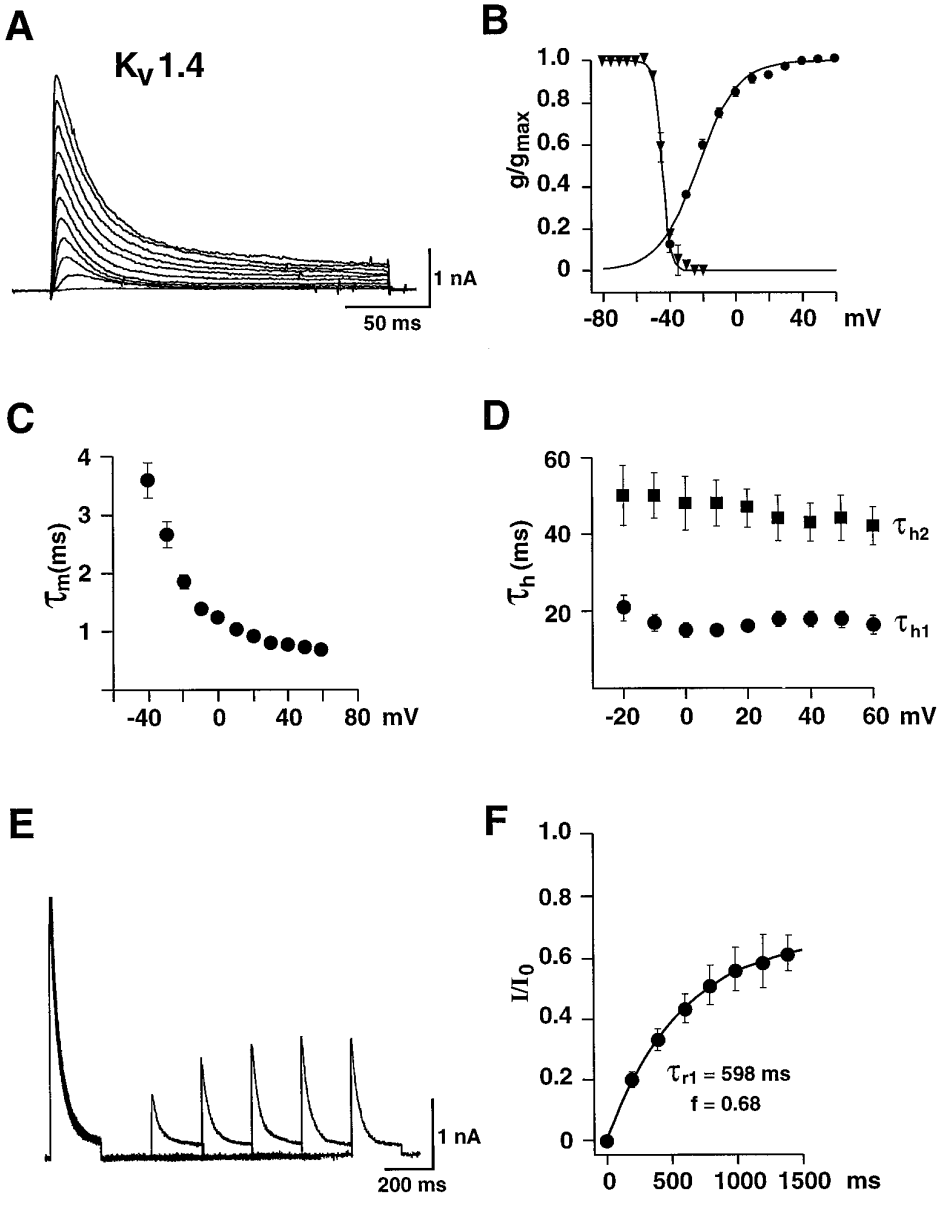

Figure 1. Properties of $K_V1.4$ currents in 293 cells. Recordings were obtained in the perforated-patch whole-cell configuration from $K_V1.4$–293 cells. *A*, Currents were elicited by 200 msec depolarizing pulses of increasing amplitudes in steps of 10 mV from a holding potential of −80 mV. *B*, Mean steady-state activation ($n = 8$) and inactivation ($n = 8$) curves of $K_V1.4$ currents were fitted with Boltzmann functions to normalized mean conductances (g/g_{max}). Steady-state inactivation of $K_V1.4$ was determined using a 1 sec prepulse to increasing potentials from −80 mV in steps of 5 mV, followed by a 200 msec test pulse to +40 mV. *C*, Voltage-dependence of mean time constants of activation (τ_m; $n = 8$) of $K_V1.4$ is shown obtained from fitting individual records of $K_V1.4$ currents with a Hodgkin–Huxley related formalism (see Materials and Methods). *D*, Voltage-dependence of mean time constants of the dominant fast component (τ_{h1}; $n = 4$) and the minor slow component (τ_{h2}; $n = 4$) of $K_V1.4$ inactivation is shown as indicated. Data were obtained from fitting individual records of $K_V1.4$ currents with a Hodgkin–Huxley related formalism with two inactivation time constants (see Materials and Methods). *E*, Recovery from inactivation of $K_V1.4$ currents. $K_V1.4$ recovery was tested by a double-pulse protocol. Two 200 msec test pulses to +40 mV were separated by increasing the interpulse interval at −80 mV in steps of 200 msec. *F*, Mean time course of initial recovery from inactivation was fitted to normalized mean data (I/I_0; $n = 5$). The data were fitted by a monoexponential function to determine time constant (τ_{r1}) and fraction (f) of initial fast recovery.

mately −50 mV. $K_V1.4$ currents inactivated rapidly with a residual steady-state current after a 200 msec depolarizing test-pulse representing ~10% of the peak current (Fig. 1*A*). Voltage-dependence of steady-state $K_V1.4$ current activation was described with a Boltzmann function; mean half-maximal (V_{50}) activation occurred at −22.6 ± 1.7 mV with a mean slope of 12.1 ± 1.2. mV ($n = 8$; Fig. 1*B*). Mean half inactivation was at −44.5 ± 0.6 mV with a mean slope of 2.3 ± 0.2 mV ($n = 8$; Fig. 1*B*).

A Hodgkin–Huxley related formalism ($I = I_0 m(t)^4 h(t)$; see Materials and Methods) with a single time constant (τ_m) for activation and two time constants (τ_{h1},τ_{h2}) for inactivation was used to fit macroscopic $K_V1.4$ currents. Within the studied voltage range of −40 to +60 mV, τ_m showed a marked voltage dependency, decreasing from a mean of 3.6 ± 0.3 msec ($n = 8$) at −40 mV to 0.7 ± 0.2 msec ($n = 8$) at +60 mV (Fig. 1*C*). In agreement with previous single-channel data demonstrating the voltage independence of transitions from the open to the inactivated state in *Shaker* K_V-channels (Zagotta and Aldrich, 1990), time constants of $K_V1.4$ inactivation showed no apparent voltage dependency between −20 to +60 mV ($n = 6$; Fig. 1*D*). Throughout this range, >70% ($I\tau_{h1}/I = 73.5 \pm 4.1\%$; $n = 12$) of a fast inactivation component ($\tau_{h1} = 16.6 \pm 0.9$ msec at +40 mV; $n = 12$) and <30% ($I\tau_{h2}/I = 26.5 \pm 4.1\%$; $n = 12$) of a slower inactivation component ($\tau_{h2} = 43.3 \pm 2.3$ msec at +40 msec; $n = 12$) contributed to $K_V1.4$ inactivation. Two distinct molecular mechanisms for K^+ channel inactivation have been described: N-type inactivation, which depends on an amino terminal inactivation domain acting rapidly as a tethered intracellular K^+ channel blocker (Hoshi et al., 1990), and C-type inactivation, which seems to involve slower structural changes at the extracellular mouth of the channel pore (Baukrowitz and Yellen, 1995, 1996). Deletion of the amino terminal of $K_V1.4$ inactivation domain [$K_V1.4\Delta110$; (Rettig et al., 1994)] removes rapid N-type inactivation of $K_V1.4$ currents and a pure C-type inactivation remains. Expression of $K_V1.4\Delta110$ in 293 cells exhibited slowly inactivating currents (data not shown). The inactivation time course was well described by a single time constant in the range of 200 msec ($\tau_h = 218 \pm 16$ msec; $n = 5$) that is

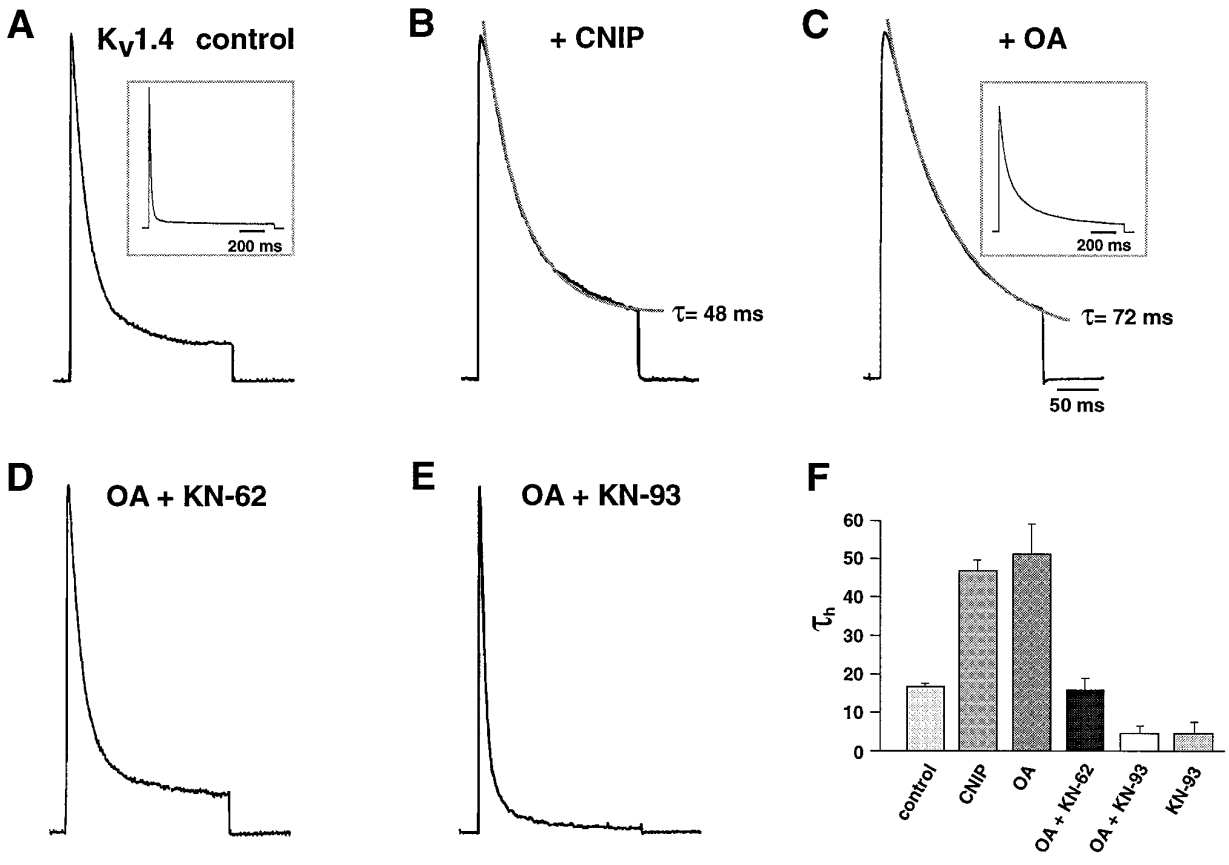

Figure 2. Modulation of $K_V1.4$ by inactivation protein phosphatases and CaMKII. *A–E*, Recordings of $K_V1.4$ currents were obtained in the perforated-patch whole-cell configuration. Current responses were elicited by a 200 msec depolarizing pulse to +40 mV from a holding potential of −80 msec from $K_V1.4$–293 cells (*A*) under control conditions, (*B*) after microinjection of 10 μM *CNIP*, (*C*) after 30 min preincubation with 100 nM *OA*, (*D*) after 30 min preincubation with 100 nM *OA* and 10 μM KN-62, (*E*) after 30 min preincubation with 100 nM *OA* and 10 μM KN-93. *Inserts* in *A* and *C* show current responses to 1 sec depolarizing pulses. In *B* and *C*, monoexponential fits of inactivation are superimposed. For comparison, currents were normalized to peak. *F*, Mean fitted time constants (τ_h) of the dominant (>70%) inactivation component of $K_V1.4$ currents recorded with the perforated-patch configuration under conditions shown in *A–E* as well as after preincubation with 10 μM KN-93. Data were obtained from four to six independent experiments.

significantly longer than the two time constants for $K_V1.4$ wild-type inactivation. It seems that at least the dominant fast inactivation component of $K_V1.4$ represents pure N-type inactivation.

It has been shown that recovery from inactivation of *Shaker* channels involves at least two processes, a fast one in the millisecond time range and a slow one, which takes several seconds for completion (Zagotta and Aldrich, 1990; Demo and Yellen, 1991; Baukrowitz and Yellen, 1995). The fast component reflects recovery from N-type inactivation, the slow one that from C-type inactivated states (Baukrowitz and Yellen, 1995). Similarly, $K_V1.4$ recovery from inactivation, determined in the perforated-patch configuration by a double pulse protocol of 200 msec depolarizing voltage steps to +40 mV separated by variable interpulse intervals at −80 mV (Fig. 1*E*), exhibited a fast and a slow component (Fig. 1*F*). Sixty-eight percent of the initial $K_V1.4$ current recovered from inactivation via the fast recovery process [fraction (f) of fast recovery = 0.68], which could be described by a single exponential with a time constant τ_{r1} of 598 msec (n = 5; Fig. 1*F*). More hyperpolarized interval pulse potentials accelerated the initial component of $K_V1.4$ recovery from inactivation saturating at potentials negative to −120 mV. The voltage dependence of the initial recovery process was described with a Boltzmann function with a mean V_{50} of −53.5 ± 1.5 mV and slope of 17.8 ± 11.2 mV (n = 3). Complete recovery of $K_V1.4$ from inactivation took up to 15 sec. The slow recovery process apparently had a time constant in the range of several seconds. Recovery of $K_V1.4\Delta110$ channels from C-type inactivation was similarly slow (τ_h = 2.4 ± 0.7 sec; n = 3). The slow recovery process showed no apparent voltage dependence. Because of this slow component of $K_V1.4$ recovery, in all pulse protocols we used interval times of 30 sec between test pulses to avoid cumulative inactivation of $K_V1.4$ currents.

Dephosphorylation accelerates $K_V1.4$ inactivation

When calcineurin (protein phosphatase 2B) was inhibited in $K_V1.4$–293 cells by microinjecting the calcineurin inhibitory peptide (CNIP, 10 μm) 1 hr before $K_V1.4$ current recordings in the perforated-patch configuration, a delayed $K_V1.4$ inactivation time course (Fig. 2*B*) was observed in comparison to controls (Fig. 2*A*). In contrast, time constants of activation were not affected by this treatment. Inactivation in the presence of CNIP could be well described with only one time constant (τ_h). Its value, 48.1 ± 2.5 msec at + 40 mV (n = 6), was similar to the slowly inactivating component τ_{h2}, which contributes <30% to the inactivation time course of $K_V1.4$ currents in controls. Preincubation of $K_V1.4$–293 cells with cyclosporin A, which blocks calcineurin via cyclophillins, also resulted in a slowed $K_V1.4$ inactivation time course (46.1+ 1.9 msec; n = 3) similar to those observed with microinjected CNIP.

Calcineurin is able to initiate a calcineurin/inhibitor-1 protein

phosphatase cascade where active calcineurin, by means of dephosphorylating an inhibitor, upregulates the activity of the calcium-independent protein phosphatase 1 [(PP1); for review, see Cohen, 1989]. PP1 activity is inhibited by nanomolar concentrations of okadaic acid (OA). To determine whether this cascade was also active in $K_V1.4$–293 cells, they were preincubated with 100 nM OA for 30 min. In the presence of this protein phosphatase blocker, $K_V1.4$ inactivation kinetics were also slow and similar to those observed with calcineurin inhibition (Fig. 2*C*). The inactivation time course of $K_V1.4$ currents could again be well described by one time constant τ_h (51 ± 8 msec at + 40 mV; $n = 6$). Fitting the inactivation time constant of $K_V1.4$ current responses to 1 sec depolarizing pulses gave similar time constants (57 ± 10 msec at + 40 mV, $n = 5$). In addition to PP1, 100 nM OA can also block PP2A, another calcium-independent protein phosphatase. PP2A has the highest affinity to this blocker and therefore can be selectively blocked with 1 nM OA (Cohen, 1989). Preincubation with 1 nM OA resulted in a less pronouced slowing of $K_V1.4$ inactivation kinetics compared with the control ($\tau_h = 30.4 \pm 2.8$; $n = 3$) suggesting that in contrast with the calcineurin/inhibitor-1 protein phosphatase cascade, PP2A plays a minor role in regulation of $K_V1.4$ inactivation kinetics.

When both the protein phosphatases and CaMKII were inhibited with 100 nM OA and 10 μM KN-62, respectively, $K_V1.4$ currents were indistinguishable from those in control cells (Fig. 2*A,D*). This showed that the effect of protein phosphatase inhibition on $K_V1.4$ inactivation was occluded completely by the simultaneous application of a CaMKII inhibitor. Furthermore, incubation of $K_V1.4$–293 cells with 100 nM okadaic acid and 10 μM KN-93, a more potent blocker of CaMKII compared with KN-62 (Sumi et al., 1991), yielded $K_V1.4$ currents, which now inactivated approximately threefold faster than $K_V1.4$ control currents ($\tau_{h1} = 4.4 \pm 0.3$ msec at + 40 mV; $n = 5$) (Fig. 2*A,E*). Similar to the results obtained in the simultaneous presence of OA and KN-93, the $K_V1.4$ inactivation time course was dominated (OA+KN-93: $I\tau_{h1}/I = 88.5 \pm 1.5\%$; $n = 5$) by a fast inactivation time constant τ_{h1} in the presence of KN-93 alone (4.2 ± 0.3 msec; $I\tau_{h1}/I = 92.9 \pm 1.0\%$; $n = 6$) (Fig. 2*F*). These data suggested tentatively that $K_V1.4$–293 cells contained a steady-state equilibrium between dephosphorylated and phosphorylated $K_V1.4$ protein altered by either blocking the calcineurin/inhibitor-1 protein phosphatase cascade or CaMKII. Apparently, an increase in the concentration of phosphorylated $K_V1.4$ protein induced by protein phosphatase blockers caused a slowing of inactivation kinetics. Conversely, a decrease in CaMKII-phosphorylated $K_V1.4$ protein induced by CaMKII blockers caused an acceleration of $K_V1.4$ inactivation kinetics. In contrast, the amplitude and kinetics of endogenous 293 currents were not effected by either inhibition of phosphatases (100 nM OA, $n = 5$) or CaMKII (10 μM KN-62; $n = 5$).

CaMKII phosphorylates $K_V1.4$ channels

CaMKII might phosphorylate one or more of the three CaMKII phosphorylation consensus sites present in the $K_V1.4$ amino terminus. Two of the motifs involving serine residues 101/102 and 123 are specific for $K_V1.4$. They do not occur in other K_V1 subfamily members (Chandy and Gutman, 1994). The third motif is related to threonine residue 191 located at equivalent positions within the amino terminal tetramerization (T) domain of all K_V1 subfamily members (Shen and Pfaffinger, 1995). Serine 123, threonine 191, and serines 101/102 were replaced with alanine by *in vitro* mutagenesis of $K_V1.4$ cDNA ($K_V1.4$ S123A, $K_V1.4$ T191A, $K_V1.4$ SS101/102AA) to generate nonfunctional CaMKII consensus sites. The cDNAs were used as templates for *in vitro* mRNA synthesis. $K_V1.4$ T191A mRNA did not express functional $K_V1.4$ channels after microinjection into 293 cells and therefore was not analyzed further. $K_V1.4$ SS101/102AA expressed only small currents with properties that were similar to wild-type $K_V1.4$ (see below). $K_V1.4$ S123A mRNA, on the other hand, expressed large currents after microinjection into 293 cells. The combined biochemical and electrophysiological characterization of $K_V1.4$ S123A provided evidence that strongly suggested that serine 123 was the CaMKII modulatory site of $K_V1.4$ (see below).

CaMKII-dependent phosphorylation of wild-type $K_V1.4$ and $K_V1.4$ S123A mutants were assayed *in vitro*. Wild-type $K_V1.4$ and $K_V1.4$ S123A mRNAs were translated into protein using a reticulocyte lysate supplemented with microsomes. The translated $K_V1.4$ proteins were subsequently incubated with purified CaMKII and γ^{32}P-ATP for biochemical phosphorylation studies. The ^{32}P-labeled phosphorylated protein material was analyzed by denaturing SDS-PAGE followed by autoradiography (Fig. 3*A*). The results showed that CaMKII had phosphorylated wild-type and $K_V1.4$ S123A proteins to a different extent. Densitometric analysis of ^{32}P-labeled $K_V1.4$ protein normalized for protein concentration and averaged over seven experiments showed that ~35% less ^{32}P-phosphate had been incorporated into $K_V1.4$ S123A than into wild-type $K_V1.4$ protein (Fig. 3*A*). Consistent with the presence of three CaMKII phosphorylation consensus sites in the $K_V1.4$ amino terminus, the data suggested that CaMKII *in vitro* phosphorylated more than one site on $K_V1.4$ protein and that one of the functional sites had been eliminated in the S123A mutation.

Wild-type $K_V1.4$ and $K_V1.4$ S123A mRNA were microinjected into 293 cells and expressed currents were recorded in the perforated-patch configuration. The wild-type $K_V1.4$ currents were indistinguishable from those elicited in stably transfected $K_V1.4$–293 cells (compare Figs. 1*A,* 3*B*). The inactivation time course of $K_V1.4$ S123A currents, on the other hand, was faster than wild type (Fig. 3*B,C*). It was well described with two time constants ($\tau_{h1} = 10.1 \pm 0.3$ msec; $\tau_{h2} = 36.4 \pm 3.7$ msec; $I\tau_{h1}/I = 88 \pm 4\%$; $n = 6$). Very similar time constants were obtained for $K_V1.4$ S123A currents inactivation in the presence of 1 μM cyclosporin A ($\tau_{h1} = 9.6 \pm 1.4$ msec; $\tau_{h2} = 37.5 \pm 1.5$ msec; $n = 5$), 100 nM OA ($\tau_{h1} = 10.5 \pm 1.3$ msec; $\tau_{h2} = 32.0 \pm 3.1$ msec; $n = 5$), and the CaMKII inhibitor KN-62 ($\tau_{h1} = 9.5 \pm 0.4$ msec; $\tau_{h2} = 30.9 \pm 1.6$ msec, $n = 3$). These data demonstrated that inhibition of the calcineurin/inhibitor-1 protein phosphatase cascade or of CaMKII with KN-62 did not affect $K_V1.4$ S123A inactivation kinetics in contrast to wild-type $K_V1.4$. In the presence of the CaMKII inhibitor KN-93, wild-type $K_V1.4$ (Figs. 2*E*, 3*D*) ($\tau_{h1} = 4.2 \pm 0.3$ msec; $\tau_{h2} = 26.0 \pm 0.6$ msec; $n = 6$) and $K_V1.4$ S123A (Fig. 3*E*) ($\tau_{h1} = 3.8 \pm 0.4$ msec; $\tau_{h2} = 26.9 \pm 1.6$ msec; $n = 4$) inactivation kinetics were similar and most rapid. In contrast, when the concentration of active CaMKII was increased by microinjecting the Ca^{2+}-independent autothiophosphorylated CaMKII (for review, see Braun and Schulman, 1995) before electrophysiological experiments, $K_V1.4$ and $K_V1.4$ S123A inactivation kinetics were markedly different (Fig. 3*F,G*). Inactivation of $K_V1.4$ was delayed in comparison with controls (Fig. 3*B,F*) and was fitted by a single inactivation time constant ($\tau_h = 38.3 \pm 3.3$ msec; $n = 6$). This τ_h was similar to that obtained after blocking the calcineurin/inhibitor-1 protein phosphatase cascade (Fig. 2*B,C*). In contrast, the time course of $K_V1.4$ S123A inactivation was not affected by microinjection of autothiophosphorylated CaMKII (Fig. 3*G*). The inactivation time

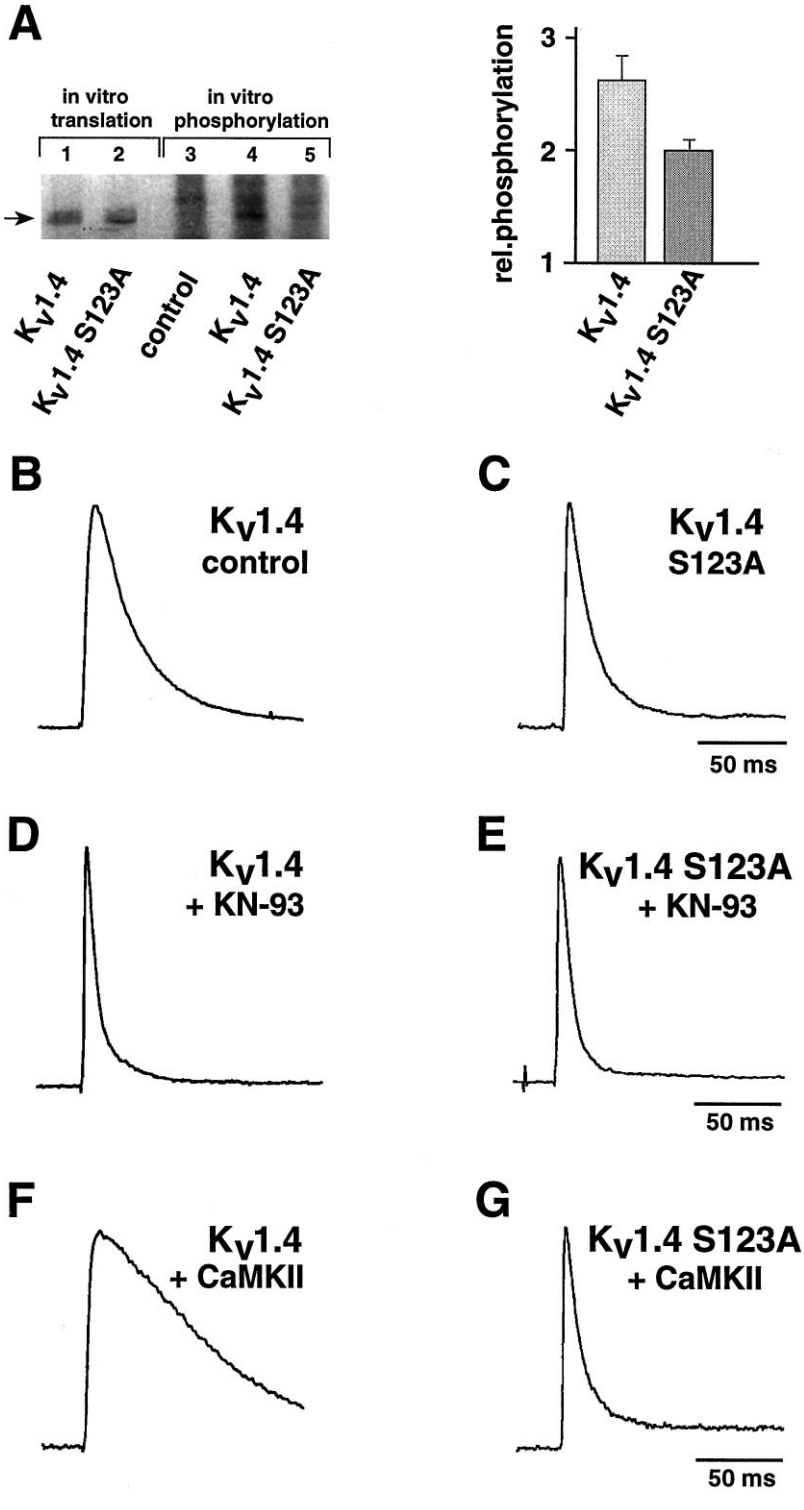

Figure 3. CaMKII phosphorylates an N-terminal $K_V1.4$ residue and slows inactivation. *A*, *In vitro* phosphorylation of $K_V1.4$ and $K_V1.4$ S123A by CaMKII. $K_V1.4$ and $K_V1.4$ S123A mRNA were translated *in vitro* in the presence of microsomes. Translation products were incubated with CaMKII and ^{32}P-γ-ATP for *in vitro* phosphorylation. Products were separated by 10% SDS-PAGE. Gels were dried and autoradiographed. *Left panel* shows autoradiogram. *Lanes 1–2, In vitro* translated, ^{35}S-labeled $K_V1.4$ and $K_V1.4$ S123A probes as indicated. *Lanes 3–5, In vitro* phosphorylated, ^{32}P-labeled control microsomal membranes (3); *in vitro* phosphorylated, ^{32}P-labeled Kv1.4 (4); *in vitro* phosphorylated, ^{32}P-labeled Kv1.4 S123 A (5). *Right panel* gives the mean relative phosphorylation by CaMKII of *in vitro* translated $K_V1.4$ and $K_V1.4$ S123A obtained from seven independent experiments. Exposure time of the autoradiographs was 12 hr. Phosphorylation intensities were scanned by phosphoimager (Fuji), analyzed by TINA 2.0 (raytest), and normalized to background. *B–G*, Recordings of $K_V1.4$ and $K_V1.4$ S123A currents were obtained in the perforated-patch whole-cell configuration from 293 cells that had been microinjected with 50 ng/μl $K_V1.4$ or $K_V1.4$ S123A mRNA as indicated, 6 hr before recording. Current responses were elicited by a 200 msec depolarizing pulse to +40 mV from a holding potential of −80 msec from cells (*B, C*) under control conditions, (*D, E*) after 30 min preincubation with 10 μM KN-93, and (*F, G*) 30 min after second microinjection with autothiophosphorylated CaMKII (2 μg/ml). For comparison, currents were normalized to peak.

course was dominated by a fast inactivation time constant (τ_{h1} = 7.9 ± 0.7 msec; $I\tau_{h1}/I$ = 87.2 ± 3.3%; n = 5) as in control recordings. The results shown in Figure 3 demonstrated that $K_V1.4$ is a substrate for CaMKII. When $K_V1.4$ was phosphorylated at the serine 123 modulatory site, $K_V1.4$-mediated currents inactivated 5–10 times slower than those mediated by dephosphorylated $K_V1.4$. In addition, a comparison of $K_V1.4$ Δ110 (Rettig et al., 1994) and $K_V1.4$ Δ110 S123A-mediated currents showed that they possessed very similar slow inactivation kinetics ($K_V1.4$ Δ110: τ_h = 218 ± 16 msec; n = 5; $K_V1.4$ Δ110 S123A: τ_h = 213 ± 33 msec; n = 5). This observation suggested that the CaMKII phosphorylation at serine 123 apparently modulated N-type and not C-type inactivation of $K_V1.4$.

$K_V1.4$ recovery from inactivation modulated by CaMKII

$K_V1.4$ currents that were recorded from $K_V1.4$–293 cells microinjected with autothiophosphorylated CaMKII recovered from inactivation twofold faster and more completely (Fig. 4*A,B*) than

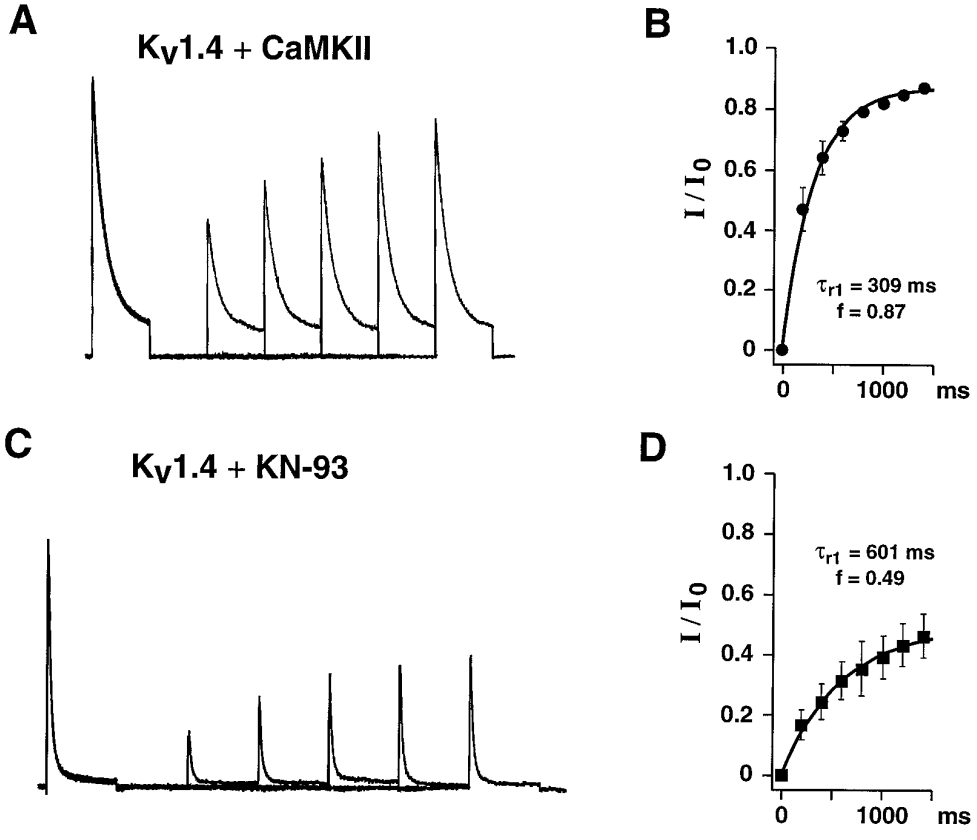

Figure 4. CaMKII phosphorylation accelerates $K_V1.4$ recovery from inactivation. Recordings of $K_V1.4$ currents were obtained in the perforated-patch whole-cell configuration from $K_V1.4$–293 cells. Recovery from $K_V1.4$ inactivation was determined by a double-pulse protocol. Current responses to two 200 msec test pulses to +40 mV separated by increasing the interpulse intervals at −80 mV in steps of 200 msec were recorded; *A*, microinjection with autothiophosphorylated CaMKII (2 μg/ml); *C*, after 30 min preincubation with 10 μM KN-93. Mean time course of recovery from inactivation was fitted to normalized mean data (I/I_O) obtained from five independent experiments, (*B*) after microinjection with autothiophosphorylated CaMKII, and (*D*) after 30 min preincubation with 10 μM KN-93. The mean time course of initial recovery was fitted by a monoexponential function to determine time constant (τ_{r1}) and fraction (f) of initial recovery.

control (Fig. 1*E,F*). Eighty-seven percent ($f = 0.87$) of the $K_V1.4$ current amplitude recovered from inactivation with a time constant τ_{r1} = 309 msec (n = 5). This suggested that most $K_V1.4$ channels in the CaMKII-phosphorylated form recovered directly from N-type inactivation and did not enter the long absorbing C-type inactivated state. In the presence of KN-93, however, initial $K_V1.4$ recovery was twofold slower, with a time constant similar to control (τ_{r1} = 601; n = 5) and recovered only to 49% with the initial fast component (Fig. 4*C,D*). Therefore, in the dephosphorylated form, ~50% of the $K_V1.4$ channels entered the long absorbing C-type inactivated state via N-type inactivation. The mean voltage dependency of the initial recovery component was not affected by CaMKII phosphorylation. In CaMKII-microinjected cells, it was described with a Boltzmann function with V_{50} at −52.9 ± 1.9 mV and a slope of 18.9 ± 1.6 mV (n = 4). With KN-93, $V50$ was −55.2 ± 1.1 mV with a slope of 15.8 ± 0.8 mV (n = 3). Initial recovery of $K_V1.4$ S123A currents from inactivation was even slower (τ_{r1} = 755 msec; n = 3), and less completely ($f = 0.41$; n = 3) suggesting that ~60% of the $K_V1.4$ S123A channels recovered through a long absorbing state. These results indicated that the modulation of $K_V1.4$ inactivation kinetics by CaMKII phosphorylation affected not only the rate of $K_V1.4$ recovery from inactivation, but also the pathway of recovery. After CaMKII phosphorylation, more $K_V1.4$ channels apparently returned directly from N-type inactivated state(s) and less entered long absorbing C-type inactivated state(s).

Macroscopic kinetics of voltage-dependent activation and the steady-state activation curve of $K_V1.4$ were not affected by CaMKII phosphorylation (Fig. 5). Steady-state activations were described by Boltzmann functions and mean V_{50} values and slopes obtained for $K_V1.4$ currents from both CaMKII-microinjected cells (V_{50} = −20.6 ± 2.0 mV; slope = 12.5 ± 1.4 mV; n = 6) and KN-93 treated cells (V_{50} = −23.7 ± 5.2 mV; slope = 6.4 ± 1.6 mV; n = 3) were similar to those obtained in control recordings. CaMKII phosphorylation, however, affected the apparent voltage dependence of $K_V1.4$ steady-state inactivation. Microinjection of CaMKII shifted the apparent voltage-dependence of steady-state inactivation of $K_V1.4$ currents by ~7 mV to more positive membrane potentials (V_{50} at −37.8 ± 1.2 mV; n = 6; Fig. 5*B*) compared with both control recordings (Fig. 1*B*) and those in the presence of KN-93 (V_{50} was at −43.2 ± 1.8 mV; n = 4; Fig. 5*D*). Similar to dephosphorylated $K_V1.4$, the V_{50} of $K_V1.4$ S123A steady-state inactivation was also at more negative potentials (V_{50} = −44.5 ± 0.6 mV; slope = 2.6 ± 0.5 mV; n = 4).

CaMKII phosphorylation modulates $K_v1.4$ cumulative inactivation

Standard voltage-clamp protocols reflect only poorly the physiological patterns of excitation occurring *in vivo*; i.e., repetitive discharge of short action potentials at varying frequencies. Under these conditions, A-type K_V channels like $K_V1.4$ are likely to undergo repetitive activation–deactivation and inactivation–recovery cycles. This is correlated with the occurrence of cummulative inactivation that involves both N-type and C-type inactivation (Baukrowitz and Yellen, 1995). To approximate physiological consequences that may be correlated with the CaMKII phosphorylation of $K_V1.4$ channels, we simulated physiological discharge patterns by stepping the membrane potential of $K_V1.4$–293 cells to +20 mV for 5 msec from interpulse potentials of −60 mV at frequencies between 1 and 100 Hz. Elicited $K_V1.4$ current amplitudes were recorded in the perforated-patch configuration. In CaMKII-microinjected $K_V1.4$–293 cells, 10 Hz stimulation induced only a small cumulative inactivation (Fig. 6*A*). After 10 consecutive pulses, ~80% of the initial $K_V1.4$ current amplitude

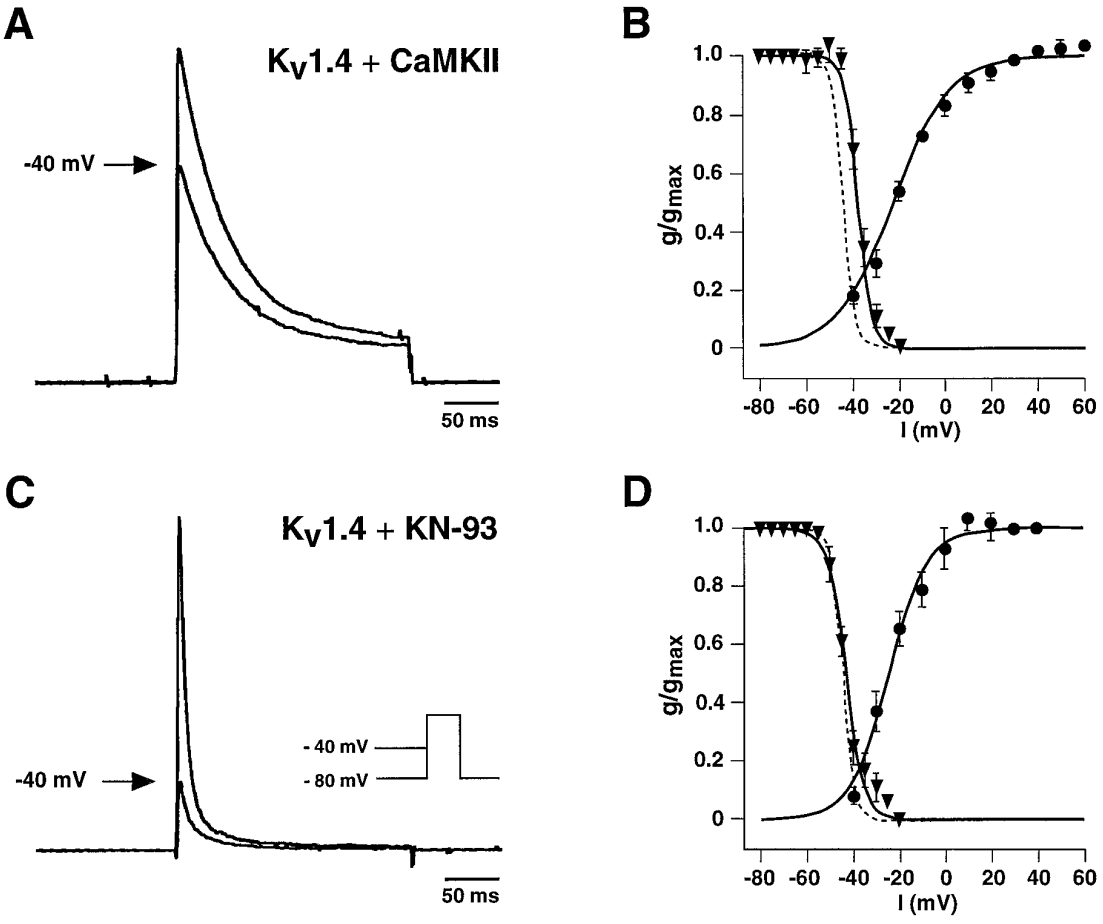

Figure 5. CaMKII phosphorylation shifts $K_V1.4$ steady-state inactivation to positive potentials. Recordings of $K_V1.4$ currents were obtained in the perforated-patch whole-cell configuration from $K_V1.4$-293 cells (*A, B*) microinjected with autothiophosphorylated CaMKII (2 μg/ml), or (*C, D*) 30 min preincubated with 10 μM KN-93. *A–C*, For steady-state inactivation, current responses were elicited by 1 sec prepulse to −80 and −40 mV (*arrows*) followed by a 200 msec test pulse to +40 msec. For comparison, currents were normalized to peak. *B–D*, Mean steady-state activation (n = 3,6) and inactivation curves (n = 4,6) of $K_V1.4$ currents were fitted with Boltzmann functions to normalized mean conductances (g/g_{max}). *Dotted lines* represent fitted steady-state inactivation under control conditions.

was still present. Throughout the studied frequency range (1–100 Hz), an acceleration of cumulative inactivation with increasing stimulation frequencies was apparent (Fig. 6*B*), but even with 100 Hz, >50% of the initial $K_V1.4$ amplitude was present after 10 pulses, demonstrating a relative resistence of CaMKII-phosphorylated $K_V1.4$ channels to cumulative inactivation. In contrast, dephosphorylated $K_V1.4$ channels obtained by either KN-93 incubation of wild-type $K_V1.4$ (Fig. 6*C,D*) or expression of $K_V1.4$ S123 channels (Fig. 6*E,F*) were sensitive to repetitive stimulation. In both cases, 10 Hz stimulation induced a significant cumulative inactivation after 10 pulses. A loss of ~80% of the initial current amplitude was observed (Fig. 6*C,E*). The increased sensitivity of dephosphorylated $K_V1.4$ to cumulative inactivation was already apparent at 1 Hz stimulation frequencies and was accentuated at higher stimulation frequencies (Fig. 6*D,F*). After 10 pulses at 100 Hz, only ~10% of the initially available $K_V1.4$ channels remained active. Thus, the frequency–dependence of $K_V1.4$ cumulative inactivation is determined markedly by CaMKII phosphorylation of $K_V1.4$ at serine 123.

Inactivation kinetics of $K_V1.4$ currents are Ca^{2+} dependent

The activation of CaMKII and calcineurin is regulated by intracellular Ca^{2+}. In contrast with calcineurin, however, CaMKII can be converted to a Ca^{2+}-independent form after autophosphorylation (Miller and Kennedy, 1986; Braun and Schulman, 1995). As we have shown, the phosphorylation status of the $K_V1.4$ modulatory site depends on the relative activities of calcineurin and CaMKII and should thus depend on the intracellular Ca^{2+}concentration. To examine this hypothesis directly, we recorded from $K_V1.4$–293 cells in the whole-cell patch-clamp configuration to dialyze the cells with different free Ca^{2+} concentrations. With 200 nM free Ca^{2+} in the pipette solution, $K_V1.4$ currents were similar to those observed in the perforated-patch configuration and showed no apparent change of inactivation kinetics throughout the course of the experiment (Fig. 7*A,E*). Accordingly, inactivation time courses could be described by double exponential functions. A fast process with a time constant τ_{h1} of 10.4 ± 1.3 msec at +40 mV (n = 6) dominated inactivation ($I\tau_{h1}/I$ = 86.3 ± 3.1%) and the minor component (>15%) had a mean time constant, τ_{h2} of 34.4 ± 2.2 msec at +40 mV (n = 6) (Fig. 7*F*). Similar time constants were determined for whole-cell patch-clamp recordings with free Ca^{2+} concentrations between 0.1 and 1 μM in the pipette solution (Fig. 2*F*). Also, steady-state activation and inactivation curves were similar to perforated-patch results (200 nM Ca^{2+}: activation, V_{50} = −23.1 ± 1.6; slope = 11.2 ± 0.6 mV; n = 8; inactivation: V_{50} =−48.7 ± 2.2

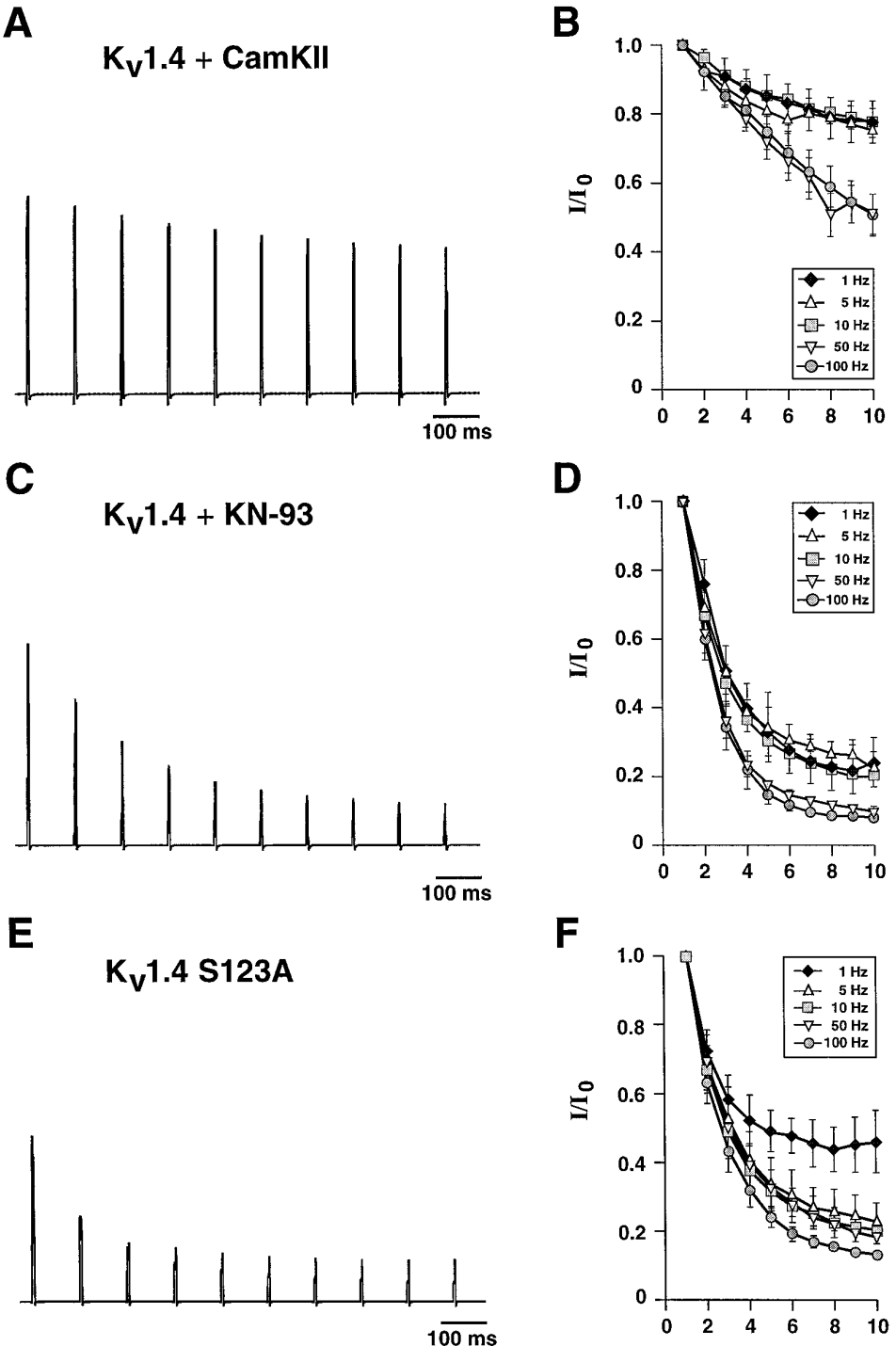

Figure 6. CaMKII phosphorylation reduces cumulative inactivation of $K_V1.4$ currents. Recordings of $K_V1.4$ currents were obtained in the perforated-patch whole-cell configuration from $K_V1.4$-293 cells (*A, B*) microinjected with autothiophosphorylated CaMKII (2 μg/ml) (*C, D*) 30 min preincubated with 10 μM KN-93, and $K_V1.4$ S123A cRNA microinjected 293 cells (*E, F*). *A, C, E*, Current responses were elicited by 10 Hz stimulations of 5 msec depolarizations to +20 mV from a holding potential of −60 mV. For comparison, currents were normalized to peak of first current response. *B, D, F*, Normalized mean current amplitudes (I/I_0; $n = 6$) elicited by 5 msec depolarizations to +20 mV from a holding potential of −60 mV with stimulation frequencies at 1, 5, 10, 50, and 100 Hz are plotted versus pulse number. *Symbols* represent stimulation frequencies as indicated.

mV, slope = 2.8 ± 0.3 mV; $n = 8$). In contrast, when the free Ca^{2+} concentration in the pipette solution was reduced to 20 nM, inactivation of $K_V1.4$ currents progressively slowed after whole-cell dialysis (Fig. 7*B*). The first $K_V1.4$ current response, which was recorded immediatedly after breaking into the cell, still exhibited fast inactivation comparable with those recorded with higher Ca^{2+} concentrations. However, the $K_V1.4$ current responses, which were subsequently recorded at 30 sec intervals, showed increasingly slower inactivation accompanied by an increase in sustained current at the end of the 200 msec pulse and an increase in total charge transfer (Fig. 7*E*). The Ca^{2+}-dependent modulation of $K_V1.4$ inactivation reached a steady-state 6–10 min after breaking into the cell for standard whole-cell recording (Fig. 7*B*). During dialysis of 20 nM free Ca^{2+}, the slowing of the $K_v1.4$ inactivation time course could be described as a continous increase of the contribution of the slowly inactivating component (τ_{h2} = 38.4 ± 1.6 msec, $n = 5$). This initially accounted for only ~12% (τ_{h2}/I = 11.8 ± 3.4%; $n = 5$) of the inactivating $K_v1.4$ current and then rose to ~65% (τ_{h2}/I = 65.0 ± 6.1%; $n = 5$). Accordingly, the contribution of the fast inactivating component (τ_{h1} = 7.8 ± 1.1 msec; $n = 5$) had decreased during 20 nM Ca^{2+} dialysis from 88 to 35%. Preincubation with KN-62 blocked the

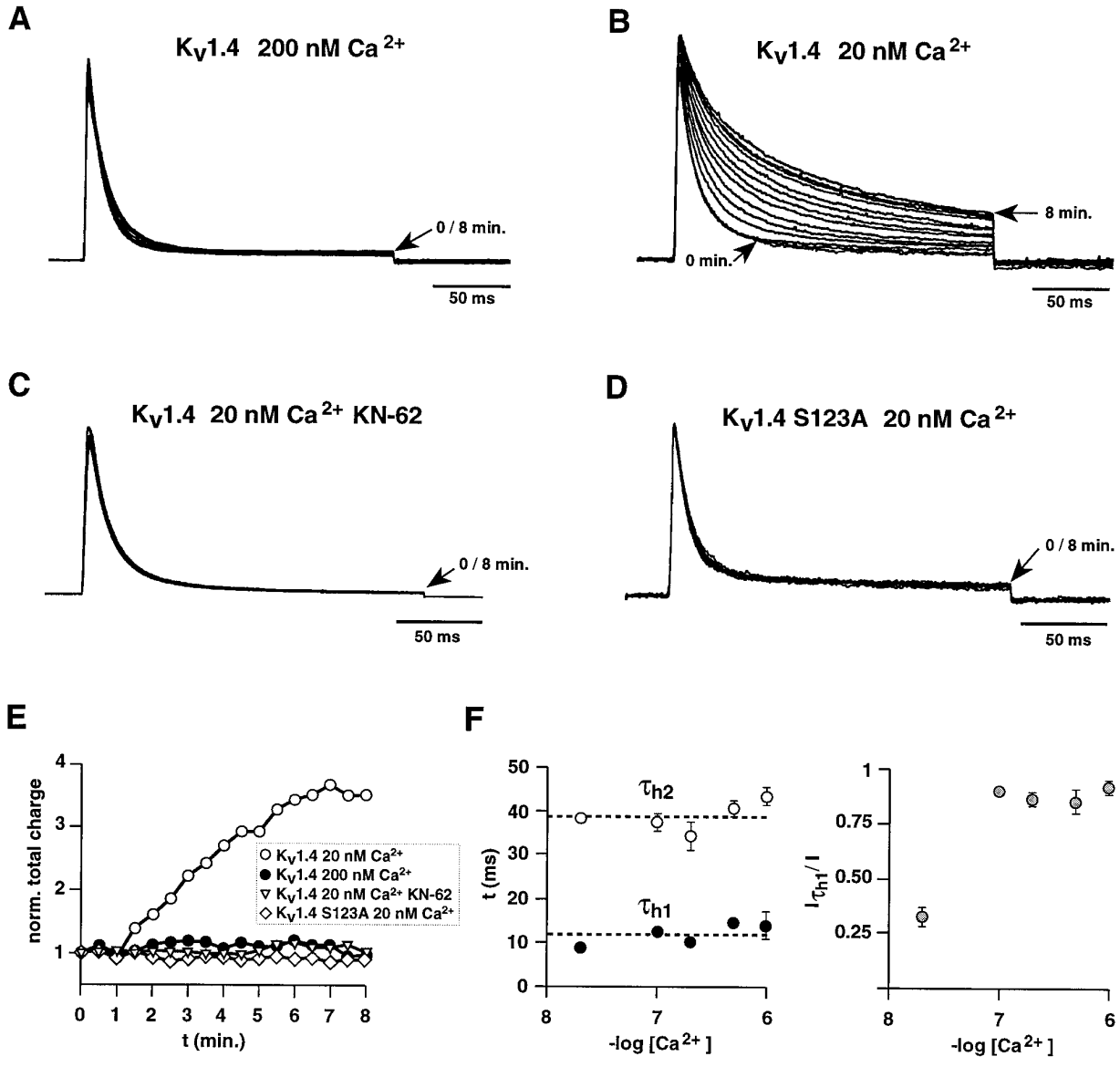

Figure 7. $K_V1.4$ inactivation kinetics are modulated by intracellular Ca^{2+} concentration. Recordings of $K_V1.4$ currents were obtained in the standard whole-cell configuration from $K_V1.4$-293 cells with (*A*) 200 nM free Ca^{2+}, (*B*) 20 nM Ca^{2+} in the pipette solution, and (*C*), 20 nM Ca^{2+} in the pipette solution after preincubation with 10 μM KN-62. *D*, Similar recordings were obtained from 293 cells expressing $K_V1.4$ S123A currents with 20 nM Ca^{2+} in the pipette solution. Currents were elicited by 200 msec test pulse to +40 mV starting immediately after breaking into the cell and subsequently in 30 sec intervals. Current responses at 0 min and 8 min as indicated (*arrows*). *E*, Normalized mean charge transfer ($n = 4$) induced by repetitive 200 msec test pulses from $K_V1.4$- and $K_V1.4$ S123A-expressing cells to +40 mV with 20 nM and 200 nM free Ca^{2+} in the pipette solution as indicated. *F, Left panel*, Mean inactivation time constants of the fast (τ_{h1}) and slow component (τ_{h2}) plotted against the free Ca^{2+} in the pipette solutions ($n = 4–8$) of $K_V1.4$ currents. *Dotted lines* represent mean time constants at all Ca^{2+}-concentrations tested. *F, Right panel*, Mean normalized contribution ($I\tau_{h1}/I$) of the fast (τ_{h1}) component to $K_V1.4$ inactivating currents. $I\tau_{h1}/I$ was plotted against the free Ca^{2+} concentration in the pipette solutions used for the whole-cell recordings ($n = 4–8$).

transition from fast to slow $K_V1.4$ inactivation with dialysis of 20 nM free Ca^{2+} solutions (Fig. 7*C,E*). When similar whole-cell patch-clamp experiments were performed with 293 cells expressing $K_V1.4$ S123A currents, no Ca^{2+} sensitivity of the time course of inactivation was observed, and the fast component of inactivation was dominant ($I\tau_{h1}/I > 85\%$) with dialysis of both 20 nM (Fig. 7*D,E*) and 200 nM free Ca^{2+} concentrations (20 nM: τ_{h1} 9.2 ± 0.3 msec; τ_{h2} 37.2 ± 2.5 msec; $I\tau_{h1}/I = 90.4 + 3.2\%$; $n = 10$). In contrast, 293 cells expressing $K_V1.4$ SS101/102AA showed similar slowing after dialysis with 20 nM free Ca^{2+} concentrations compared with $K_V1.4$ wild-type ($n = 3$) indicating that serines 101/2 are not involved in Ca^{2+} dependend modulation of $K_V1.4$. These results suggested that the transition from fast to slow $K_V1.4$ current inactivation observed with 20 nM Ca^{2+} dialysis depended on the presence of CaMKII-phosphorylated $K_V1.4$ channels. Accordingly, the transition was blocked by preincubation with the CaMKII inhibitor KN-62 and apparently favored by the inhibition of the calcineurin/inhibitor-1 protein phosphatase cascade (Fig. 2*B,C*). The most likely explanation for these observations is that the balance between calcineurin and CaMKII activitities in $K_V1.4$–293 cells was shifted at 20 nM Ca^{2+} in favor of the Ca^{2+} independent autophosphorylated form of CaMKII, and consequently the concentration of CaMKII-phosphorylated $K_V1.4$

was increased. Our data provide strong evidence that the Ca^{2+} sensitivity of $K_V1.4$ inactivation kinetics is an expression of the dynamic equilibrium between CaMKII-phosphorylated and calcineurin/protein phosphatase 1 dephosphorylated $K_V1.4$.

DISCUSSION

CaMKII phosphorylation of a $K_V1.4$ amino-terminal site modulates inactivation kinetics

In this study, we have given biochemical and electrophysiological evidence that the Ca^{2+}/CaMKII phosphorylated an important modulatory site of $K_V1.4$ channels, located at serine 123 within the amino-terminal cytoplasmic domain. Furthermore, we have shown that this site is dephosphorylated by the Ca^{2+}-dependent calcineurin/inhibitor-1 protein phosphatase cascade. CaMKII-phosphorylation of $K_v1.4$ has several functional consequences of $K_V1.4$ activity. First, the time course of inactivation of CaMKII-phosphorylated $K_V1.4$ channels (τ_h = 40–50 msec) (Fig. 3) is slowed by approximately one order of magnitude in comparison to that of dephosphorylated $K_V1.4$ channels (τ_h = 4–8 msec) (Fig. 3). Second, CaMKII-phosphorylated $K_V1.4$ showed an accelerated recovery from inactivation, a reduced propensity to enter long absorbing inactivated states, and a reduced tendency to undergo cumulative inactivation when stimulated with a train of action potential-like short depolarizations. Third, the voltage-dependent steady-state inactivation of CaMKII-phosphorylated $K_V1.4$ channels was shifted to more positive potentials by ~7 mV. This might increase a $K_V1.4$ window current in the subthreshold range of between −50 and −30 mV.

Under control conditions in the perforated-patch configuration, $K_V1.4$ currents had properties that were typical for dephosphorylated $K_V1.4$; i.e., a dominant fast inactivating component, slow and incomplete initial recovery, and steady-state inactivation with a V_{50} at −45 mV. This indicated that $K_V1.4$ was present in $K_V1.4$–293 cells predominantly in the dephosphorylated form. The concentration of CaMKII-phosphorylated $K_V1.4$ in 293 cells was increased by either microinjection of autothiophosphorylated CaMKII or by inhibition of calcineurin/protein phosphatase 1. Dialysis of $K_V1.4$–293 cells with pipette solutions containing 20 nM free Ca^{2+} had a similar effect on $K_V1.4$ inactivation kinetics as pharmacological inhibition of protein phosphatases. Both effects were occluded by the preincubation with the CaMKII inhibitors KN-62 or KN-93. These results suggest that in the 293 cellular enviroment $K_V1.4$ channels exist in a steady-state equilibrium of CaMKII-phosphorylated and dephosphorylated forms. In aggreement with this notion are the properties of the currents mediated by $K_V1.4$ S123A, which cannot be phosphorylated at the serine 123 modulatory site. These channels were locked in the fast inactivating mode and were not affected by microinjection of autothiophosphorylated CaMKII, protein phosphatase inhibitors, or dialysis with 20 nM free Ca^{2+} solutions.

CaMKII phosphorylation of $K_V1.4$ modulates functional coupling of N- and C-type inactivation and frequency-dependent cumulative inactivation

Two principally different inactivation mechanisms have been identified for *Shaker*-related A-type channels. One is mediated by the amino-terminal inactivating "ball" domain acting as a intracellular tethered blocker of the open channel and has been termed N-type inactivation (Hoshi et al., 1990). The second mechanism, named C-type, is mediated by C-terminal domains and involves conformational changes at the extracellular mouth of the pore (Choi et al., 1991; Hoshi et al., 1991; Lopez-Barneo et al., 1993). Both types of inactivation can influence each other in a cooperative manner (Baukrowitz and Yellen, 1995, 1996). When the amino-terminal "ball" domain is deleted, e.g., in $K_V1.4$ Δ110 (Rettig et al., 1994), $K_V1.4$ channels inactivate only via C-type inactivation (τ_h = 213 msec). Comparison of the inactivation kinetics of CaMKII-phosphorylated $K_V1.4$ channels with that of $K_V1.4$ Δ110 shows that the former is still significantly faster than the latter. Also, the S123A mutation did not affect the time constant of C-type inactivation ($K_V1.4$ Δ110 S123A: τ_h = 218 msec). This suggests that CaMKII-phosphorylation of the modulatory site at serine 123 may exert its effects on N-type inactivation of $K_V1.4$. It is likely, however, that CaMKII phosphorylation influences C-type inactivation indirectly by reducing the functional coupling between N-type and C-type inactivated states. As pointed out by Baukrowitz and Yellen (1995), a short depolarizing pulse drives *Shaker* A-type K channels into N-type inactivation. From this state, they have two main pathways: they either recover directly via an open state (Ruppersberg et al., 1991) to resting states with rate λ or enter the long absorbing C-type inactivated state (Demo and Yellen, 1991) with rate μ. Therefore, the time constant for the fast phase of recovery is $\tau_{r1} = [(\lambda + \mu)^{-1}$ and the fraction (f) of channels recovering via the fast route is $f = \lambda/(\lambda + \mu)$ (Baukrowitz and Yellen, 1995)]. In the dephosphorylated state of $K_V1.4$, these parameters are f = 0.5 and τ_{r1} = 600 msec (Fig. 4*D*), i.e., both pathways have an equal rate of ~0.8 sec^{-1}. In comparison, the rate of recovery from C-type inactivation determined with the $K_V1.4$Δ110 mutant is ~0.4 sec^{-1}. This comparison suggests that dephosphorylated $K_V1.4$ channels are bound to accumulate in the C-type inactivated state via N-type inactivation. In contrast, the fraction of CaMKII-phosphorylated $K_V1.4$ channels recovering directly from N-type inactivation is almost 90% (f = 0.87), with a time constant of 300 msec (Fig. 4*B*). This predicts an accelerated rate λ of $K_V1.4$ recovery from N-type inactivation (2.8 sec^{-1}) and a reduced rate μ for entering the C-type inactivated state from N-type inactivation (0.5 sec^{-1}). The latter is only slightly faster than the rate of leaving the C-type inactivated state (0.4 sec^{-1}). This suggests that only a minor fraction of CaMKII phosphorylated $K_V1.4$ channels can accumulate in the C-type inactivated state via N-type inactivation. Thus, CaMKII phosphorylation of $K_V1.4$ is likely to interfere with the functional interplay of N-type and C-type inactivation. CaMKII phosphorylation of $K_V1.4$ shifted the frequency-dependence of cumulative inactivation, induced by short repetitive depolarizations, toward higher stimulation frequencies (Fig. 6). Only dephosphorylated $K_V1.4$ channels showed an effective cumulative inactivation at low stimulation frequencies. This is in agreement with previous results that cumulative inactivation of *Shaker* A-type channels is most effective when N-type and C-type inactivation are both present and strongly coupled (Baukrowitz and Yellen, 1995).

Different localizations of modulatory phosphorylation sites in *Shaker*-related A-type channels

It has been proposed from detailed kinetic analysis of *Shaker* channel inactivation combined with *in vitro* mutagenesis that N-type inactivation follows a "ball and chain" mechanism in which the ball is tethered to a flexible chain (Hoshi et al., 1990). Most likely, long-range electrostatic interactions are essential for the on-rate of inactivation (Murrell-Lagnado and Aldrich, 1993). They are apparently dominated by positive charges clustered within the inactivation domain and negative charges near or at the ball receptor region (Isacoff et al., 1991; Yool and Schwarz, 1995). Changes in net charge induced by phosphorylation in the ball

region or other channel domains therefore are likely to affect inactivation kinetics. Covarrubias et al. (1994) showed for the cloned human A-type K_V channel, hK_V3.4 that PKC-dependent phosphorylation within the inactivation domain completely eliminates N-terminal inactivation. Conversely, Drain et al. (1994) demonstrated for *Shaker* K_V channels that the phosphorylation of a C-terminal consensus site by PKA induces an acceleration of the macroscopic and microscopic transition from the open channel into the inactivated state. Therefore, the effect of phosphorylation on inactivation kinetics might be critically dependent on the localization of the phospho-acceptor in the channel protein. The CaMKII phosphorylation site in K_V1.4 is obviously not part of the inactivation ball or ball receptor region, but rather is situated in the putative chain domain. It is possible that the density of negative charges near or at the CaMKII phosphorylation site might affect the flexibility of the "chain" connecting the inactivation ball with the core of the protein. Alternatively, phosphorylation at serine 123 might weaken the electrostatic ball–receptor interaction.

A role in synaptic frequency detection for CaMKII-dependent phosphorylation of K_V1.4?

It is likely that K_V1.4 channels are an *in vivo* substrate for CaMKII. In rat brain, K_V1.4 channels may contribute, like *Shaker* channels in Drosophila, to action potential repolarization (Pardo et al., 1992). They are predominantly targeted to presynaptic compartments (Sheng et al., 1992, 1993; Veh et al., 1995) where CaMKII (Braun and Schulman, 1995) and several protein phosphatases like calcineurin and protein phosphatase 1 are also abundant (Liu et al., 1994). The balance between CaMKII and the calcineurin/inhibitor-1 protein phosphatase cascade activities is known to regulate a number of pre- and postsynaptic key proteins (for review, see Schulman, 1995), including AMPA receptors (McGlade-McCulloh et al., 1993; Mulkey et al., 1994; Wyllie and Nicoll, 1994). It is an attractive possibility that CaMKII phosphorylation of K_V1.4 channels contributes to the described CaMKII-induced shift of frequency-dependent properties of central synapses to higher discharge rates (Bear, 1995; Chapman et al., 1995; Mayford et al., 1995). Although it is not clear how CaMKII is involved in synaptic frequency detection, several studies favor the calmodulin trapping mechanism by autophosphorylated CaMKII as a good candidate (Meyer et al., 1992; Dosemeci and Albers, 1996). CaMKII-dependent modulation of K_V1.4 inactivation kinetics might be an important additional factor. A synapse that makes use of K_V1.4 activity, would require higher firing frequencies to drive CaMKII-phosphorylated K_V1.4 channels into cumulative inactivation and, in turn, to increase the presynaptic action-potential duration facilitating Ca^{2+} entry (for review, see Byrne and Kandel, 1996). Only functional analysis of synapses, however, will clarify the relevance of CaMKII-dependent regulation of native fast-inactivating K channels for neural excitability.

REFERENCES

Baukrowitz T, Yellen G (1995) Modulation of K^+ current by frequency and external (K^+): a tale of two inactivation mechanisms. Neuron 15:951–960.

Baukrowitz T, Yellen G (1996) Use-dependent blockers and exit rate of the last ion from the multi-ion pore of a K^+ channel. Science 271:653–656.

Bear MF (1995) Mechanism for a sliding synaptic modification threshold. Neuron 15:1–4.

Bliss TVP, Collingridge GL (1993) A synaptic model of memory: long-term potentiation in the hippocampus. Nature 361:31–39.

Braun AP, Schulman H (1995) The multifunctional calcium/calmodulin dependent protein kinase: from form to function. Annu Rev Physiol 57:417–445.

Byrne JH, Kandel ER (1996) Presynaptic facilitation revisited: state and time dependence. J Neurosci 16:425–435.

Chandy KG, Gutman GA (1994) Voltage-gated potassium channels. In: CRC Handbook of receptors and channels (North, PA, ed), pp. 1–71. Boca Raton: CRC.

Chapman PF, Frenguelli BG, Smith A, Chen CM, Silva AJ (1995) The alpha-Ca2+/calmodulin kinase II: a bidirectional modulator of presynaptic plasticity. Neuron 14:591–597.

Chen C, Okayama H, Cohen PT (1987) High-efficiency transformation of mammalian cells by plasmid DNA. Mol Cell Biol 7:2745–2752.

Choi KL, Aldrich RW, Yellen G (1991) Tetraethylammonium blockade distinguishes two inactivation mechanisms in voltage-activated K^+ channels. Proc Natl Acad Sci USA 88:5092–5095.

Cohen P (1989) The structure and regulation of protein phosphatases. Annu Rev Biochem 58:453–508.

Covarrubias M, Wei A, Salkoff L, Vyas TB (1994) Elimination of rapid potassium channel inactivation by phosphorylation of the inactivation gate. Neuron 13:1403–1412.

Demo SD, Yellen G (1991) The inactivation gate of the Shaker K^+ channel behaves like an open-channel blocker. Neuron 7:743–753.

Dosemeci A, Albers RW (1996) A mechanism for synaptic frequency detection through autophosphorylation of CaM kinase II. Biophys J 70:2493–2501.

Drain P, Dubin AE, Aldrich RW (1994) Regulation of Shaker K^+ channel inactivation gating by the cAMP-dependent protein kinase. Neuron 12:1097–1109.

Hamill OP, Neher ME, Sakmann B, Sigworth F (1981) Improved patch-clamp techniques for high-resolution current recording from cells and cell-free membrane patches. Pflügers Arch 391:85–100.

Ho SN, Hunt HD, Horton RM, Pullen JK, Pease LR (1989) Site-directed mutagenesis by overlap extention using the polymerase chain reaction. Gene 77:51–59.

Holmes TC, Fadool DA, Levitan IB (1996) Tyrosine phosphorylation of the Kv1.3 potassium channel. J Neurosci 16:1581–1590.

Hoshi T, Zagotta WN, Aldrich RW (1990) Biophysical and molecular mechanisms of Shaker potassium channel inactivation. Science 250:533–538.

Hoshi T, Zagotta WN, Aldrich RW (1991) Two types of inactivation in Shaker K^+ channels: effects of alterations in the carboxy-terminal region. Neuron 7:547–556.

Huang X-Y, Morelli AD, Peralta EG (1993) Tyrosine kinase-dependent suppression of a potassium channel by the G protein-coupled m1 muscarinic receptor. Cell 75:1145–1156.

Huang X-Y, Morelli AD, Peralta EG (1994) Molecular basis of a cardiac potassium channel stimulation by protein kinase A. Proc Natl Acad Sci USA 94:624–628.

Ikeda SR, Soler F, Zuhlke RD, Joho RH, Lewis DL (1992) Heterologous expression of the human potassium channel Kv2.1 in clonal mammalian cells by direct cytoplasmic microinjection of cRNA. Pflügers Arch 422:201–203.

Isacoff EY, Jan YN, Jan LY (1991) Putative receptor for the cytoplasmic inactivation gate in the Shaker K^+ channel. Nature 353:86–90.

Jonas EA, Kaszmarek LK (1996) Regulation of potassium channels by protein kinases. Curr Opin Neurobiol 6:318–323.

Kandel ER, Schwartz JH, Jessell TM (1991) Principles of neural science, 3rd Ed. New York: Elsevier.

Karin M, Haslinger A, Holtgreve H, Richards RI, Krauter P, Westphal HM, Beato M (1984) Characterization of DNA sequences through which cadmium and glucocorticoid hormones induce human metallothionein-II_A gene. Nature 308:513–519.

Lev S, Moreno H, Martinez R, Canoll P, Peles E, Musacchio JM, Plowman GD, Rudy B, Schlessinger J (1995) Protein tyrosine kinase PYK2 involved in Ca(2+)-induced regulation of ion channel and MAP kinase functions. Nature 376:737–745.

Liu J-P, Sim ATR, Robinson PJ (1994) Calcineurin inhibition of dynamin I GTPase activity coupled to nerve terminal depolarization. Science 265:970–973.

Lopez-Barneo J, Hoshi T, Heinemann SH, Aldrich RW (1993) Effects of external cations and mutations in the pore region on C-type inactivation of Shaker potassium channels. Receptors Channels 1:61–71.

Mayford M, Wang J, Kandel ER, O'Dell TJ (1995) CaMKII regulates the frequency-response function of hippocampal synapses for the production of both LTD and LTP. Cell 81:891–904.

McGlade-McCulloh E, Yamamoto H, Tan S-E, Brickey DA, Soderling TR (1993) Phosphorylation and regulation of glutamate receptors by calcium/calmodulin-dependent protein kinase II. Nature 362:640–642.

Meyer T, Hanson PI, Stryer L, Schulman H (1992) Calmodulin trapping by calcium-calmodulin dependent protein kinase. Science 256:1199–1202.

Miller SG, Kennedy MB (1986) Regulation of brain type II Ca2+/calmodulin-dependent protein kinase by autophosphorylation: a Ca^{2+}-triggered molecular switch. Cell 44:861–870.

Moreno H, Kentros C, Bueno E, Weiser M, Hernandez A, Vega-Saenz de Miera E, Ponce A, Thornhill W, Rudy B (1995) Thalamocortical projections have a K^+ channel that is phosphorylated and modulated by cAMP-dependent protein kinase. J Neurosci 15:5486–5501.

Mulkey RM, Endo S, Shenolikar S, Malenka RC (1994) Involvement of a calcineurin/inhibitor-1 phosphatase cascade in hippocampal long-term depression. Nature 369:486–488.

Murrell-Lagnado RD, Aldrich RW (1993) Interactions of amino terminal domains of Shaker K channels with a pore blocking site studied with synthetic peptides. J Gen Physiol 102:949–975.

Pardo LA, Heinemann SH, Terlau H, Ludewig U, Lorra C, Pongs O (1992) Extracellular K^+ specifically modulates a rat brain K+ channel. Proc Natl Acad Sci USA 89:2466–2470.

Rae J, Cooper K, Gates P, Watsky M (1991) Low access resistance perforated patch recordings using amphotericin B. J Neurosci Methods 37:15–26.

Rettig J, Heinemann SH, Wunder F, Lorra C, Parcej DN, Dolly JO, Pongs O (1994) Inactivation properties of voltage-gated K^+ channels altered by presence of beta-subunit. Nature 369:289–294.

Ruppersberg JP, Frank R, Pongs O, Stocker M (1991) Cloned neuronal IK(A) channels reopen during recovery from inactivation. Nature 353:657–660.

Sanger F, Nicklen S, Coulson AR (1977) DNA sequencing with chain-terminating inhibitors. Proc Natl Acad Sci USA 74:5463–5467.

Schulman H (1995) Protein phosphorylation in neuronal plasticity and gene expression. Curr Opin Neurobiol 5:375–381.

Shen V, Pfaffinger P (1995) Molecular recognition and assembly seqeunces involved in the subfamily-specific assembly of voltage-gated K^+ channel subunit proteins. Neuron 14:625–633.

Sheng M, Tsaur ML, Jan YN, Jan LY (1992) Subcellular segregation of two A-type K^+ channel proteins in rat central neurons. Neuron 9:271–284.

Sheng M, Liao YJ, Jan YN, Jan LY (1993) Presynaptic A-current based on heteromultimeric K^+ channels detected *in vivo*. Nature 365:72–75.

Stühmer W, Ruppersberg JP, Schröter KH, Sakmann B, Stocker M, Giese KP, Perschke A, Baumann A, Pongs O (1989) Molecular basis of functional diversity of voltage-gated potassium channels in mammalian brain. EMBO J 8:3235–3244.

Sumi M, Kiuchi K, Ishikawa T, Ishii A, Hagiwara M, Nagatsu T, Hidaka H (1991) The newly synthesized selective Ca2+/calmodulin dependent protein kinase II inhibitor KN-93 reduces dopamine contents in PC12h cells. Biochem Biophys Res Commun 181:968–975.

Veh RW, Lichtinghagen R, Sewing S, Wunder F, Grumbach IM, Pongs O (1995) Immunohistochemical localization of five members of the Kv1 channel subunits: contrasting subcellular locations and neuron-specific co-localizations in rat brain. Eur J Neurosci 7:2189–2205.

Wilson GG, O'Neill CA, Sivaprasadarao A, Findlay JBC, Wray D (1994) Modulation by protein kinase A of a cloned rat brain potassium channel expressed in *Xenopus* oocytes. Pflügers Arch 428:186–193.

Wyllie DJA, Nicoll RA (1994) A role for protein kinases and phosphatases in the Ca2+-induced enhancement of hippocampal AMPA receptor-mediated synaptic responses. Neuron 13:635–643.

Yool AJ, Schwarz TL (1995) Interactions of the H5 pore region and hydroxylamine with N-type inactivation in the Shaker K^+ channel. Biophys J 68:448–458.

Zagotta WN, Aldrich RW (1990) Voltage-dependent gating of *Shaker* A-type potassium channels in *Drosophila* muscle. J Gen Physiol 95:29–60.

Zucker RS (1993) Calcium and transmitter release. J Physiol (Paris) 87:25–36.